www.editada.org

International Journal of Combinatorial Optimization Problems and Informatics, 18(1), 2027, 71-86. ISSN: 2007-1558.
https://doi.org/10.61467/2007.1558.2027.v18i1.1495

Stability Analysis of Linear Models of Connected Cruise Control Systems via a Delay Lyapunov Matrix-Based Criterion

Alejandro Castaño[1], Carlos Cuvas-Castillo[2], Jesús-Patricio Ordaz-Oliver[1], Omar Sandre-Hernandez[1,3]

[1] Área Académica de Informática y Electrónica, Universidad Autónoma del Estado de Hidalgo, Hidalgo, México.

[2] Departamento de Ingeniería Mecánica Automotriz, Universidad Politécnica de Pachuca, Hidalgo, México.

[3] Secretaría de Ciencia, Humanidades, Tecnología e Innovación (SECIHTI).

Email address(es): alejandro_castano@uaeh.edu.mx, carlos.cuvas@upp.edu.mx, jesus_ordaz@uaeh.edu.mx, omar_sandre@uaeh.edu.mx

✉Corresponding author: Alejandro Castaño

Abstract. The stability analysis of Connected Cruise Control systems with communication delays requires stability criteria that provide finite necessary and sufficient conditions. This paper presents the first application of a finite stability criterion based on the delay Lyapunov matrix to linear Connected Cruise Control models. The proposed analysis combines the semianalytical computation of the delay Lyapunov matrix with a finite-dimensional verification criterion to reconstruct previously reported stability regions through a finite number of operations. Moreover, the minimum discretization level is introduced as a new characterization of the controller parameter space, providing additional information on the computational effort required for finite stability verification. Finally, controller gains selected from the certified stability regions are implemented on a connected vehicle platform, demonstrating the practical feasibility of the resulting controller under the operating conditions considered. This work establishes a practical link between recent advances in finite stability criteria for time-delay systems and the analysis of Connected Cruise Control.

Keywords: Connected Cruise Control; Connected Vehicle Systems; Time-delay systems; delay Lyapunov matrix; Finite stability criterion; Lyapunov–Krasovskii functional.

Article information
Received: Jun 22, 2026
Accepted: Aug 01, 2026

1. Introduction

The sustained growth in transportation demand has driven the development of new control strategies aimed at improving traffic efficiency, safety, and roadway capacity. Increasing traffic density promotes congestion, increases travel times and fuel consumption, raises pollutant emissions, and elevates the risk of accidents associated with human driving behavior (Treiber & Kesting, 2013; Rajamani, 2012). In this context, Intelligent Transportation Systems (ITS) have incorporated vehicle-to-vehicle (V2V) communication technologies, giving rise to Connected Vehicle Systems (CVSs), in which vehicles cooperate through information exchange to improve the collective behavior of traffic flow.

Among the control strategies developed for Connected Vehicle Systems, Connected Cruise Control (CCC) has emerged as one of the most representative cooperative approaches for the longitudinal control of vehicle platoons (Orosz, 2016; Juárez et al., 2018). Unlike conventional car-following strategies, CCC exploits V2V communication to incorporate position and velocity information from multiple preceding vehicles into the control law. As a result, each controller has access to a broader description of the traffic state, improving longitudinal vehicle following, mitigating the propagation of traffic perturbations, and promoting coordinated platoon motion (Orosz, 2016).

The performance of CCC, however, depends critically on the timely availability of the exchanged information. Wireless communication, data processing, and packet update mechanisms inevitably introduce delays into the control loop, modifying the longitudinal dynamics of the system and potentially compromising platoon stability (Orosz, 2016). Since these delays are an inherent feature of CVSs, they must be explicitly incorporated into the dynamic model to accurately describe the system behavior. Consequently, stability criteria capable of explicitly accounting for communication delays are essential for the analysis and design of Connected Cruise Control strategies.

From the perspective of stability analysis, the explicit inclusion of delays fundamentally changes the problem formulation. Unlike delay-free systems, the current system dynamics depend explicitly on both the present state and the state at previous time instants, substantially increasing the mathematical complexity of the stability analysis. Consequently, classical Lyapunov methods cannot be applied directly, and specialized tools for time-delay systems become necessary. Among them, the Lyapunov–Krasovskii functional framework has provided a rigorous theoretical foundation for the development of stability conditions and analysis methods for linear time-delay systems (Kharitonov, 2013; Gomez et al., 2019; Mondié et al., 2022).

The analysis based on Lyapunov–Krasovskii functionals with prescribed derivative reveals that the stability characterization of linear time-delay systems depends on a matrix-valued function that plays a role analogous to that of the Lyapunov matrix for delay-free systems (Kharitonov, 2013). This function, known as the delay Lyapunov matrix, constitutes the central element for formulating stability conditions and has motivated numerous developments concerning its properties, computation, and application to the analysis of time-delay systems (Gomez et al., 2019; Mondié et al., 2022). Within this framework, several finite stability criteria have recently been developed to verify necessary and sufficient stability conditions through a finite number of operations. Gomez et al. (2019) introduced the first finite criterion based on the delay Lyapunov matrix, demonstrating that these conditions could be verified by a finite number of operations. Independently, Alexandrova and Belov (2025) developed an alternative finite criterion based on Gu's discretization method, leading to a significantly less conservative estimate of the minimum discretization level required for numerical verification.

Despite these advances, the Connected Cruise Control literature and the literature on finite stability criteria based on the delay Lyapunov matrix have evolved largely independently. While the reference models for the stability analysis of connected vehicle platoons continue to rely on criteria developed before the emergence of the finite approaches currently available (Orosz, 2016; Juárez et al., 2018), recent developments in the delay Lyapunov matrix have led to stability criteria whose numerical implementation is computationally feasible for a broad class of time-delay systems. Nevertheless, these advances have not yet been incorporated into the stability analysis of Connected Cruise Control. Consequently, the possibility remains open to analyze classical CCC configurations using a finite necessary and sufficient stability criterion, numerically reconstruct previously reported stability regions, and characterize the minimum discretization level required to certify stability through a finite number of operations.

Within this context, this work applies the finite stability criterion proposed by Alexandrova and Belov (2025) to the analysis of linear CCC models with communication delays. To this end, the delay Lyapunov matrix is computed using the semianalytical method, the criterion matrix is efficiently constructed using the algorithm proposed by Cuvas-Castillo et al. (2019), and its positive definiteness conditions are verified numerically. On this basis, the finite criterion is employed to reconstruct stability regions previously reported in the literature and to provide a new characterization of the controller parameter space through the minimum discretization level required to certify the necessary and sufficient stability conditions. Finally, controller gains selected from this analysis are implemented on a connected vehicle platform to demonstrate the feasibility of controller implementation under the operating conditions considered.

The main contributions of this work can be summarized as follows. First, the finite stability criterion based on the delay Lyapunov matrix is applied for the first time to the analysis of linear Connected Cruise Control models, establishing a connection between recent developments in time-delay systems theory and a classical problem in cooperative connected vehicle control. Second, previously reported stability regions are reconstructed through a finite verification procedure, and the minimum discretization level is introduced as a new characterization of the controller parameter space, providing additional information on the computational effort required for stability certification. Finally, the feasibility of experimentally implementing controller gains selected from the finite stability analysis is demonstrated on a connected vehicle platform.

The remainder of this paper is organized as follows. Section 2 presents the nonlinear and linearized dynamic models of the Connected Cruise Control configurations considered in this work. Section 3 introduces the finite stability criterion based on the delay Lyapunov matrix and presents the mathematical elements required for its numerical implementation. Section 4 presents the application of the criterion to the Connected Cruise Control configurations together with the experimental evaluation of the implemented controller on a connected vehicle platform. Finally, Section 5 summarizes the main conclusions and discusses directions for future research.

Notation: *Throughout the paper,* $\mathbb{R}^n$ *denotes the* n*-dimensional Euclidean space. The spaces of continuous and piecewise continuous functions defined on the interval* $[-h,0]$ *and taking values in* $\mathbb{R}^n$ *are denoted by* $\mathcal{C}([-h,0],\mathbb{R}^n)$ *and* $\mathcal{PC}([-h,0],\mathbb{R}^n)$ *respectively. For vectors and matrices,* $\|\cdot\|$ *denotes the Euclidean norm and its induced matrix norm. For a function* φ *the supremum norm over the delay interval is defined by* $\|\varphi\|_h := \sup_{\theta\in[-h,0]} \|\varphi(\theta)\|$. *The transpose of a matrix* A *is denoted by* $A^\top$, *while* I_n *and* 0_n *denote the identity matrix of dimension* n *and a zero matrix of appropriate dimensions, respectively. The operators* $\mathrm{vec}(\cdot)$ *and* $\mathrm{vec}^{-1}(\cdot)$ *denote matrix vectorization and its inverse operation, respectively, and* $\otimes$ *denotes the Kronecker product. For a symmetric matrix* Q, $\lambda_{\min}(Q)$ *denotes its smallest eigenvalue. The notation* $Q > 0$

indicates that Q is positive definite. The symbol $\lceil \cdot \rceil$ denotes the ceiling function. Block matrices with (i,j)-th entry A_{ij} are compactly represented by $\{A_{ij}\}_{i,j=1}^{N}$. Unless otherwise stated, all matrices are assumed to have compatible dimensions.

2. Connected Cruise Control Dynamics

The longitudinal dynamics of a connected vehicle system equipped with a Connected Cruise Control (CCC) strategy constitute the modeling framework considered in this work. Its general configuration is illustrated in Fig. 1. Through vehicle-to-vehicle (V2V) wireless communication, each vehicle has access to position and velocity information from other vehicles, extending the information available for control beyond that provided by conventional car-following strategies. In this context, delays associated with information transmission and processing modify the longitudinal dynamics of the system and must therefore be explicitly incorporated into its mathematical model (Orosz, 2016).

This work considers two Connected Cruise Control configurations: a leader–follower system and a three-vehicle platoon. These configurations are commonly adopted as benchmark cases for analyzing the influence of communication delays and vehicle interactions on traffic flow stability (Orosz, 2016; Juárez et al., 2018). Their linearized models are developed in the following subsections and provide the basis for the stability analysis presented throughout this work.

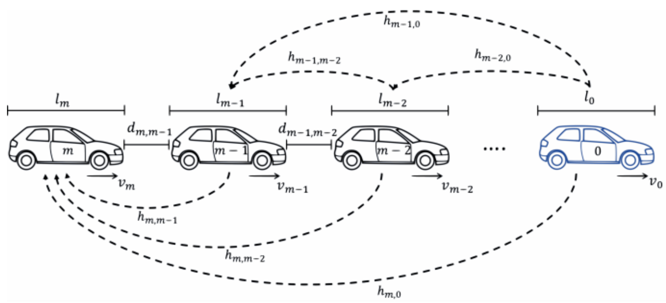

Fig. 1 Connected Vehicle Systems.

2.1 Nonlinear Vehicle-Following Model

Following the Connected Cruise Control model developed by Orosz (2016) and the time-domain formulation presented by Juárez et al. (2018), Connected Cruise Control can be interpreted as a consensus problem in which vehicles exchange information to coordinate their velocities and regulate inter-vehicle spacing. Consequently, the dynamics of each vehicle depend not only on local measurements but also on information received from preceding connected vehicles through vehicle-to-vehicle (V2V) communication.

The longitudinal dynamics of a platoon composed of m connected vehicles are described by a nonlinear time-delay system. Following the model proposed by Orosz (2016), the dynamics of the $i-th$ vehicle are represented by a kinematic equation governing the inter-vehicle spacing and a dynamic equation describing the longitudinal velocity. Communication delays explicitly account for the transmission and processing of the information employed by the Connected Cruise Control strategy. The resulting model is given by

$$\begin{aligned} \dot{d}_{i,i-1}(t) &= v_{i-1}(t) - v_i(t) \\ \dot{v}_i(t) &= \alpha_{i,i-1}\left(V_i\left(d_i\left(t-h_{i,i-1}\right)\right) - v_i\left(t-h_{i,i-1}\right)\right) + \sum_{j=0}^{i-1}\gamma_{i,j}\beta_{i,j}\left(v_j\left(t-h_{i,j}\right) - v_i\left(t-h_{i,j}\right)\right) \end{aligned} \tag{1}$$

where $d_{i,i-1}(t)$ and $v_i(t)$ denote the inter-vehicle spacing and the longitudinal velocity of the $i-th$ vehicle, respectively. The control gains $\alpha_{i,i-1}$ and $\beta_{i,j}$ weight the contributions of the optimal velocity function and the relative velocity with respect to connected preceding vehicles. Moreover, $\gamma_{i,j}$ defines the V2V communication topology by identifying the vehicles that exchange information within the CCC strategy, whereas $h_{i,j}$ represents the delays associated with information transmission and processing (Orosz, 2016).

In the expression (1), the optimal velocity function $V_i(d_i(t-h_{i,j-1}))$ plays a central role in the Connected Cruise Control model by determining the desired vehicle speed as a function of the inter-vehicle spacing. Unlike control strategies based on predefined speed references, the model considered in this work computes the target velocity through an optimal velocity function (OVF), which establishes a relationship between the available spacing to the preceding vehicle and the desired speed (Orosz, 2016). In general, the OVF can be expressed as

$$V(d)=\begin{cases} 0, & \text{si } d<d_{stop}, \\ F(d), & \text{si } d_{stop}\le d\le d_{go}, \\ V_{max} & \text{si } d>d_{go}, \end{cases}$$

This expression represents the general structure of an optimal velocity function. When the inter-vehicle spacing is smaller than d_{stop}, the desired speed remains zero. Conversely, when the spacing exceeds d_{go}, the desired speed reaches its maximum value V_{max}. Between these limits, the desired speed varies continuously with the inter-vehicle spacing, defining a smooth transition between stop-and-go traffic and free-flow conditions (Orosz, 2016).

Several functions have been proposed in the literature to describe this transition region. In this work, the cosine-based optimal velocity function introduced by Orosz (2016) is adopted because it provides a smooth transition between stop-and-go traffic and free-flow conditions while preserving continuity and differentiability over the entire operating range,

$$F(d)=\frac{V_{max}}{2}\left[1-\cos\left(\pi\frac{d-d_{stop}}{d_{go}-d_{stop}}\right)\right].$$

The optimal velocity function naturally defines the uniform traffic flow conditions of the vehicle platoon. Under this operating regime, all vehicles travel at a constant speed while maintaining constant inter-vehicle spacing with respect to their predecessors. This regime corresponds to an equilibrium condition of the nonlinear system and defines the operating point about which the linear model employed in the stability analysis is derived (Orosz, 2016; Juárez et al., 2018). Consequently, the equilibrium speed and inter-vehicle spacing satisfy the relation,

$$v^{*}=V(d^{*}),$$

where $d^{\star}$ denotes the equilibrium inter-vehicle spacing and $v^{\star}$ the corresponding equilibrium speed of the traffic flow. For every value of $d^{\star}$, the optimal velocity function uniquely determines the corresponding equilibrium speed, thereby defining a continuous family of steady-state operating conditions that serves as the starting point for the linearized models developed in the following subsections.

2.2 Linearized Leader–Follower Dynamics

Following the linear formulation presented by Juárez et al. (2018), deviation variables are introduced with respect to the equilibrium inter-vehicle spacing $d^{\star}$ and the equilibrium speed $v^{\star}$. For the leader–follower configuration, these variables are defined as

$$\begin{aligned} \tilde{d}_{1,0}(t) &= d_{1,0}(t)-d^{*}, \\ v_1(t) &= v_1(t)-v^{*}, \end{aligned}$$

where $\tilde{d}_{1,0}(t)$ denotes the deviation of the inter-vehicle spacing from its equilibrium value, whereas $\tilde{v}_1(t)$ represents the deviation of the follower vehicle velocity from the uniform equilibrium speed. Expressing the nonlinear model in terms of these variables and linearizing it about the uniform equilibrium yields a second-order linear time-delay system. Defining the state vector as

$$x_1(t)=\begin{bmatrix}\tilde{d}_{1,0}(t)\\ \tilde{v}_1(t)\end{bmatrix},$$

the system dynamics can be written as

$$x_1(t)=A_{0,1}x_1(t)+A_{1,0}x_1(t-h_{1,0}) \tag{2}$$

with

$$A_{0,1}=\begin{bmatrix}0 & -1\\ 0 & 0\end{bmatrix},\quad A_{1,0}=\begin{bmatrix}0 & 0\\ \alpha_{1,0}V'(d^{*}) & -\alpha_{1,0}-\beta_{1,0}\end{bmatrix}.$$

The structure of the system matrices reflects the interaction mechanisms considered by the Connected Cruise Control strategy. In particular, the gains $\alpha_{1,0}$ and $\beta_{1,0}$ weight the contributions of the optimal velocity function and the velocity information received from the leader vehicle, respectively. Moreover, $V'(d^{\star})$ denotes the local slope of the optimal velocity function evaluated at the equilibrium point, whereas $h_{1,0}$ represents the communication delay associated with information transmission and processing within the CCC strategy (Orosz, 2016; Juárez et al., 2018).

Consequently, the control gains $\alpha_{1,0}$ and $\beta_{1,0}$ are treated as the design parameters throughout the stability analysis presented in this work. Their influence on the system stability is investigated using the finite stability criterion introduced in Section 3, which enables the verification of the necessary and sufficient stability conditions through a finite number of operations.

2.3. Three-Vehicle Connected Cruise Control Configuration

To represent the interactions arising in a vehicle platoon, this work considers a three-vehicle Connected Cruise Control configuration. This configuration constitutes the smallest system capable of simultaneously capturing the information propagation and dynamic coupling that characterize the CCC strategy while maintaining a level of complexity suitable for stability analysis (Orosz, 2016; Juárez et al., 2018).

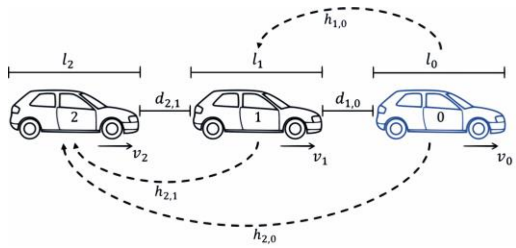

Fig. 2 Traffic systems with delays consisting of 3 connected vehicles.

The structure of the considered configuration is illustrated in Fig. 2, where the leader vehicle transmits velocity information to the follower vehicles through vehicle-to-vehicle (V2V) communication and defines the equilibrium speed $v^\star$. The analysis is carried out around the uniform traffic flow equilibrium described in Subsection 2.1. Accordingly, deviation variables associated with the inter-vehicle spacings and the follower vehicle velocities are introduced (Juárez et al., 2018),

$$x(t)=\begin{bmatrix} x_1(t) \\ x_2(t) \end{bmatrix}=\begin{bmatrix} \tilde{d}_{1,0}(t) \\ \tilde{v}_1(t) \\ \tilde{d}_{2,1}(t) \\ \tilde{v}_2(t) \end{bmatrix}=\begin{bmatrix} d_{1,0}(t)-d^\star \\ v_1(t)-v^\star \\ d_{2,1}(t)-d^\star \\ v_2(t)-v^\star \end{bmatrix}.$$

Expressing the nonlinear model in terms of these variables and linearizing it about the equilibrium yields a fourth-order linear time-delay system. Defining the state vector as (x(t)), the system dynamics can be written as

$$\dot{x}(t)=A_0x(t)+A_1x(t-h)\,. \tag{3}$$

It is further assumed that the communication and processing delays are identical, namely, $h_{1,0}=h_{2,0}=h_{2,1}=h$. This assumption allows the system dynamics to be represented by a single equivalent delay without altering the interaction structure among the vehicles in the platoon. The resulting model is therefore characterized by the matrices A_0 and A_1, whose expressions are given below (Juárez et al., 2018)

$$A_0=\begin{bmatrix} 0 & -1 & 0 & 0 \\ 0 & 0 & 0 & 0 \\ 0 & 1 & 0 & -1 \\ 0 & 0 & 0 & 0 \end{bmatrix},\quad A_1=\begin{bmatrix} 0 & 0 & 0 & 0 \\ \alpha_{1,0}V'(d^*) & -\alpha_{1,0}-\beta_{1,0} & 0 & 0 \\ 0 & 0 & 0 & 0 \\ 0 & \beta_{2,1} & \alpha_{2,1}V'(d^*) & -\alpha_{2,1}-\beta_{2,1}-\beta_{2,0} \end{bmatrix}. \tag{4}$$

The control gains $\alpha_{i,j}$ and $\beta_{i,j}$ determine the dynamic coupling between the vehicle velocities and the inter-vehicle spacings within the platoon. Consequently, these parameters are treated as the design variables in the stability analysis developed throughout this work.

3 Finite Stability Condition via the Delay Lyapunov Matrix

The models developed in the previous section belong to the class of linear time-delay systems, whose stability can be analyzed within the framework of Lyapunov–Krasovskii functionals with prescribed derivative and the theory of the delay Lyapunov matrix, which extends the classical Lyapunov theory for delay-free systems (Kharitonov, 2013; Gomez et al., 2019). A comprehensive review of the evolution of these results can be found in Mondié et al. (2022). This section presents only the mathematical elements required to introduce the finite stability criterion employed in the subsequent stability analysis of the linear Connected Cruise Control models.

3.1 Delay Lyapunov Matrix

The delay Lyapunov matrix, represented by a continuous matrix-valued function $U(\tau)$ defined over the delay interval, constitutes the fundamental mathematical object upon which the stability criteria employed in this work are constructed. Unlike the classical Lyapunov matrix, $U(\tau)$ explicitly incorporates the temporal dependence introduced by the delay and provides a convenient framework for expressing stability conditions for linear time-delay systems (Kharitonov, 2013; Gomez et al., 2019). Its formal definition is recalled below.

Definition 1 *(Kharitonov, 2013) Given a symmetric matrix $W \in \mathbb{R}^{n\times n}$, a continuous function $U : [-h, h] \to \mathbb{R}^{n\times n}$ is said to be the* ***delay Lyapunov matrix*** *of system $\dot{x}(t) = A_0x(t) + A_1x(t-h)$ if it satisfies the following set of properties:*

- *Continuity property*

$$U \in \mathcal{C}\left(\mathbb{R}, \mathbb{R}^{n\times n}\right).$$

- *Dynamic property for $\tau > 0$*

$$\frac{d}{d\tau}U(\tau) = U(\tau)A_0 + U(\tau-h)A_1$$

- *Symmetry property*

$$U(\tau) = U^{\top}(-\tau),\ \ \tau \in [-h, h].$$

- *Algebraic property*

$$-W = U(0)A_0 + A_0^{\top}U(0) + A_1^{\top}U(h) + U(-h)A_1.$$

The characteristic roots of the system are determined by its characteristic equation (Bellman & Cooke, 1963). Denoting by $\Lambda = \det(sI_n - A_0 - A_1e^{-sh})$ the set of characteristic roots, the system is said to satisfy the Lyapunov condition if, for every root $s \in \Lambda$, the relation $-s \notin \Lambda$ holds. Under this condition, the delay Lyapunov matrix exists, is unique, and can be constructed by means of a semianalytical procedure (Kharitonov, 2013).

For the class of systems considered in this work, the delay Lyapunov matrix is computed using the semianalytical method developed by Kharitonov (2013). This procedure transforms the defining properties of $U(\tau)$ into a finite-dimensional boundary-value problem, allowing the delay Lyapunov matrix to be obtained through the solution of a system of ordinary differential equations.

In particular, $U(\tau)$ is obtained as

$$U = \mathrm{vec}^{-1}(\mathcal{U}),$$

where $\mathcal{U} = \mathrm{vec}(U)$ is given by

$$\mathcal{U}(\tau) = \mathcal{E}_1 e^{\tau L}\mathcal{U}_0, \quad \tau \in [0, h],$$

with $\mathcal{W}_1 = \mathrm{vec}(W)$, and where the matrices involved in the semianalytical formulation are defined as

$$\begin{aligned}
\mathcal{E}_1 &= \begin{bmatrix} I_{n^2} & \mathbb{O}_{n^2\times n^2} \end{bmatrix},\ L = \begin{bmatrix} I_n \otimes A_0 & I_n \otimes A_1 \\ -A_1^T \otimes I_n & -A_0^T \otimes I_n \end{bmatrix}, \\
\mathcal{U}_0 &= \left(M + Ne^{Lh}\right)^{-1}\begin{bmatrix} 0_{n^2} \\ -\mathcal{W}_1 \end{bmatrix}, \\
M &= \begin{bmatrix} I_{n^2} & \mathbb{O}_{n^2\times n^2} \\ A_0^T \otimes I_n + I_n \otimes A_0 & I_n \otimes A_1 \end{bmatrix},\ N = \begin{bmatrix} \mathbb{O}_{n^2\times n^2} & -I_{n^2} \\ A_1^T \otimes I_n & \mathbb{O}_{n^2\times n^2} \end{bmatrix}
\end{aligned}.$$

The construction of $U(\tau)$ enables the formulation of stability criteria that depend exclusively on the delay Lyapunov matrix. Among them, the finite stability criterion proposed by Alexandrova and Belov (2025) constitutes the main analytical tool employed in this work to investigate the stability of both the leader–follower configuration and the three-vehicle platoon.

3.2 Finite Stability Criterion Based on the Delay Lyapunov Matrix

The following finite stability criterion, taken from Alexandrova and Belov (2025), results from the synthesis of the delay Lyapunov matrix approach and Gu's discretized Lyapunov functional method, leading to a finite necessary and sufficient stability criterion formulated in terms of the delay Lyapunov matrix. In accordance with the terminology adopted in the delay Lyapunov matrix literature (Gomez et al., 2019; Mondié et al., 2022; Alexandrova and Belov, 2025), the term ***finite stability criterion*** refers to a stability criterion whose necessary and sufficient conditions can be verified through a finite number of mathematical operations. The theorem is stated below together with the definitions required for its implementation.

Theorem 1 *(Alexandrova and Belov , 2025) System* $\dot{x}(t) = A_0 x(t) + A_1 x(t-h)$ *is exponentially stable if and only if the Lyapunov condition holds and*

$$\mathcal{K}_{N^\star} = \left\{ U\left(\frac{(j-i)h}{N^\star} \right) \right\}_{i,j=0}^{N^\star} > 0,$$

with

$$N^\star = \left\lceil \sqrt{\frac{\hat{\alpha} h^3 (2M_1 + hM_2)}{3\lambda_{\min}(W)}} \right\rceil,$$

where

$$M_1 = \max_{s\in[0,h]} \| A_1^\top U''(s) \|,$$

$$M_2 = \max_{s\in[0,h]} \| A_1^\top U''(s) A_1 \|,$$

$$\hat{\alpha} = \| A_0 \| + \| A_1 \|.$$

Theorem 1 provides a necessary and sufficient stability condition through the verification of the positive definiteness of a finite-dimensional matrix constructed from the delay Lyapunov matrix. The dimension of this matrix is determined by the minimum discretization level $N^\star$, which depends exclusively on the system bounds established by the criterion itself. This formulation constitutes the basis of the parametric stability analysis developed in the following section.

The numerical implementation of the criterion is carried out using an efficient version of the matrix construction procedure based on the algorithm proposed by Cuvas-Castillo et al. (2019). This algorithm identifies repeated evaluations of the matrix exponential required by the semianalytical method, thereby reducing the computational cost associated with constructing the criterion matrix without altering the mathematical formulation of the criterion.

4 Results and Discussion

This section presents the application of the finite stability criterion (Theorem 1) to the leader–follower and three-vehicle platoon configurations of the CCC model. The objective is to reproduce the stability regions previously reported by Juárez et al. (2018) using the finite stability criterion and to extend the analysis by determining the minimum discretization level required at each stable point in the controller parameter space.

The numerical implementation was carried out in MATLAB R2024a. For each parameter combination, the delay Lyapunov matrix associated with $W = I_n$ was computed using the semianalytical method based on the matrix exponential. The block matrices required by the finite stability criterion were then constructed using the efficient algorithm proposed by Cuvas-Castillo et al. (2019), and their positive definiteness was verified by means of a Cholesky factorization.

For both configurations, the equilibrium inter-vehicle spacing was set to $d^\star = 20\text{m}$, with $d_{stop} = 5\text{m}$, $d_{go} = 35\text{m}$, and a maximum speed of $V_{max} = 30\text{m/s}$, according to the optimal velocity function adopted in the model. These values correspond to an equilibrium speed of $v^\star = 15\text{m/s}$ and a local slope of the optimal velocity function equal to $V'(d^\star) = \frac{\pi}{2}$. Unless otherwise stated, all computations assume a uniform communication delay of $h = 0.4\ s$.

The controller parameter space was explored over a uniform 160×160 grid. For each parameter combination, the minimum discretization level $N^\star$ was determined, after which the positive definiteness of the corresponding criterion matrix was verified. The analysis begins with the leader–follower configuration to identify stable controller gains, which are subsequently employed in the study of the three-vehicle platoon.

4.1 Stability Analysis of the Leader–Follower Configuration

The finite stability criterion is applied to the leader–follower model defined by equation (2). The objective of this analysis is to identify controller gains that will subsequently be employed in the three-vehicle platoon configuration. To this end, the controller parameter space $(\alpha_{1,0}, \beta_{1,0})$ is explored over the domain $[-1,4] \times [-1,4]$ using a uniform 160×160 grid, and the finite stability criterion is evaluated for each parameter combination.

4.1.1 Stability Region Characterization

The stability region obtained using the finite stability criterion is shown in Fig. 3. This region identifies the combinations of controller gains $(\alpha_{1,0}, \beta_{1,0})$ that guarantee the stability of the leader–follower configuration and provides the basis for controller gain selection.

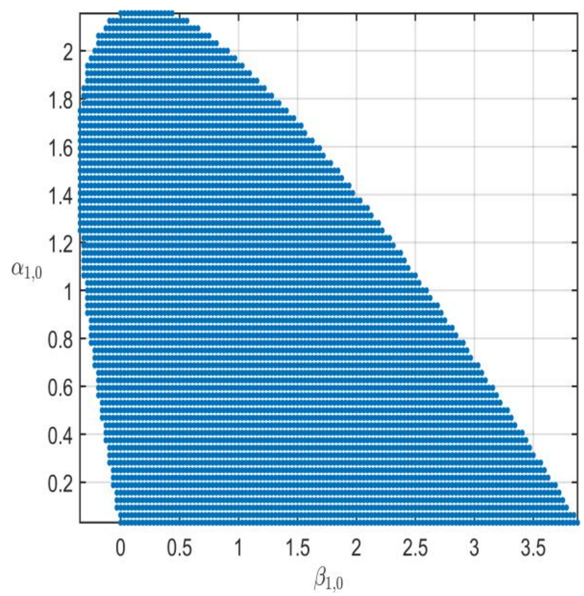

Fig. 3. Stability region of the leader--follower model in the parameter space $(\boldsymbol{\beta_{1,0}}, \boldsymbol{\alpha_{1,0}})$.

Although the stability region identifies the admissible controller gains, not all stable operating points require the same computational effort for stability verification. This additional information is provided by the minimum discretization level $N^{\star}$, whose distribution over the controller parameter space is analyzed in the following subsection.

4.1.2 Finite Stability Verification Map

The minimum discretization level map shown in Fig. 4 reveals that the computational effort required to verify the finite stability criterion is not uniform throughout the stable region. While a large portion of the controller parameter space can be certified using relatively small values of $N^{\star}$, other regions require substantially higher discretization levels. This result demonstrates that system stability and the computational effort required to certify it constitute distinct properties.

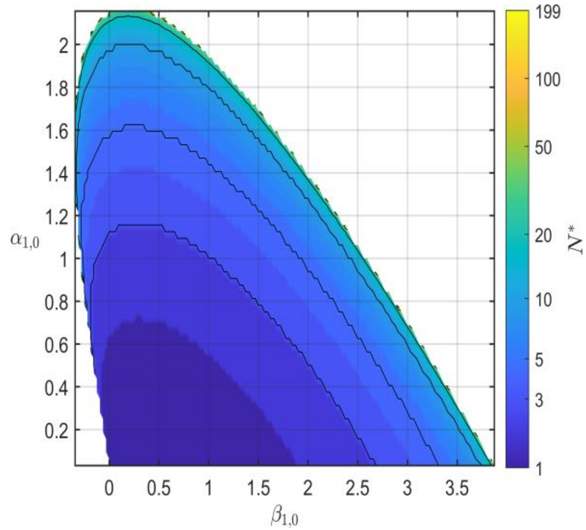

Fig. 4. Minimum discretization level $N^*$for finite verification of the stability conditions in the leader--follower

The $N^\star$ map complements the stability region by quantifying the minimum discretization level required to certify the stability of each point in the controller parameter space. Consequently, it provides a quantitative characterization of the computational effort associated with the finite stability criterion and establishes a reference for the analysis of higher-dimensional configurations, such as the three-vehicle platoon considered in the following subsection.

4.1.3 Statistical Distribution of the Minimum Discretization Level

The statistical distribution of the minimum discretization level is summarized in Fig. 5 and Table 1. The histogram shows that most stable controller gain combinations can be certified using relatively small values of $N^\star$, whereas large discretization levels occur only within a limited portion of the stable region.

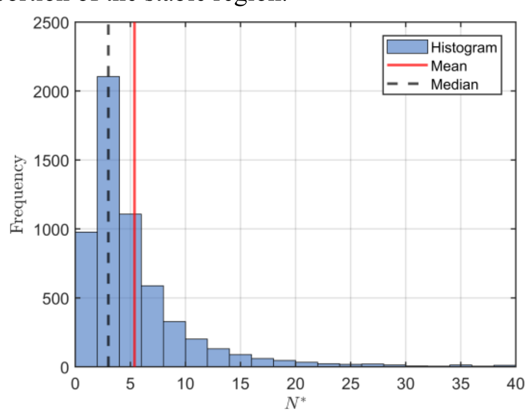

Fig. 5. Distribution of the minimum discretization level N^* for the leader--follower model.

The statistics reported in Table 1 support this observation. Although the maximum value reaches $N^\star$, the median is equal to 3 and the average value remains low, indicating that large discretization levels are confined to localized regions of the stable parameter space.

Taken together, the stability region, the $N^\star$ map, and its statistical distribution provide a comprehensive characterization of the finite stability criterion over the controller parameter space of the leader–follower configuration. These results establish the reference for the analysis of the complete three-vehicle platoon, where the previously reported stability region is reproduced and the analysis is extended through the characterization of the minimum discretization level.

4.2 Stability Analysis of a Three-Vehicle Connected Platoon

The finite stability criterion is next applied to the linearized three-vehicle platoon model defined by equation (3) with matrices expressed by (4). The controller gains for the first follower are selected from the leader–follower analysis, resulting in $\alpha_{1,0} = 0.6$ and $\beta_{1,0} = 0.7$, whereas $\beta_{2,1} = 0.7$ is adopted from the configuration proposed by Juárez et al. (2018). Under these conditions, the analysis is conducted in two stages. First, the stability regions previously reported in the literature are reproduced. Subsequently, the minimum discretization level required by the finite stability criterion is characterized.

4.2.1 Finite Verification of Previously Reported Stability Regions

Figure 6 shows that the finite stability criterion completely reproduces the stability regions previously reported by Juárez et al. (2018). The agreement between both regions confirms that the finite criterion preserves the previously established stability domain while providing stability certification through a finite verification procedure.

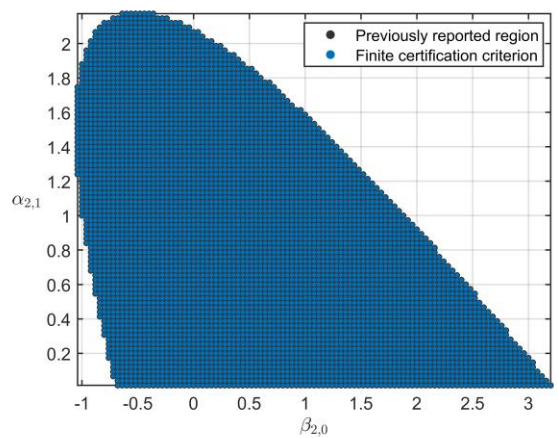

Fig. 6. Recovery of the previously reported stability region using the finite-dimensional verification criterion.

This result confirms the stability regions adopted as reference for the three-vehicle platoon configuration and establishes the basis for analyzing the minimum discretization level required by the finite stability criterion at each point within the stable region.

4.2.2 Finite Stability Verification Map of the Connected Platoon

Once the stability regions have been reproduced, the analysis is extended by computing the minimum discretization level $N^\star$ associated with each point of the stable region (Fig. 7). The resulting map characterizes the distribution of $N^\star$ over the controller parameter space and complements the classical stability analysis by incorporating information on the computational effort required to certify each controller gain combination.

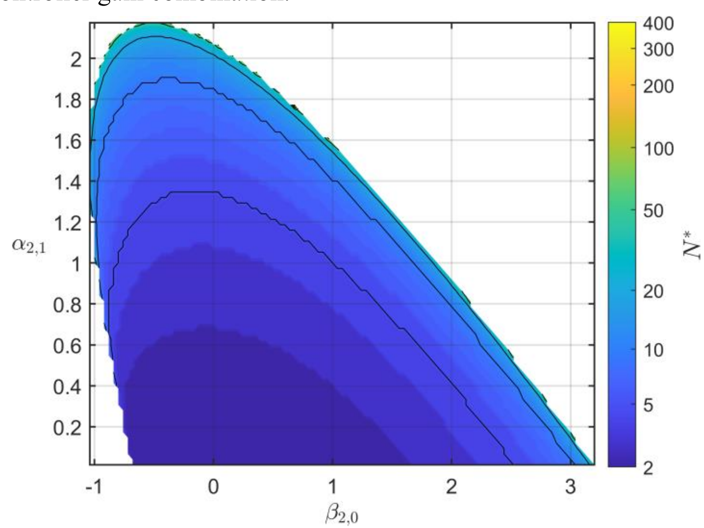

Fig. 7. Minimum discretization level N^* for finite verification of the stability conditions in the three-vehicle platoon.

The map shows that the distribution of $N^\star$ remains nonuniform throughout the stable region and that the maximum discretization levels are higher than those observed for the leader–follower configuration. Nevertheless, a substantial portion of the stable parameter space continues to require only moderate discretization levels. The overall distribution of these values is summarized statistically in the following subsection.

4.2.3 Statistical Distribution of the Minimum Discretization Level

The statistical distribution of the minimum discretization level is summarized in Fig. 8 and Table 1. Although the maximum value of $N^{\star}$ increases with respect to the leader–follower configuration, the histogram shows that most stable controller gain combinations can still be certified using relatively small discretization levels. Large values of $N^{\star}$ occur only within localized regions of the controller parameter space.

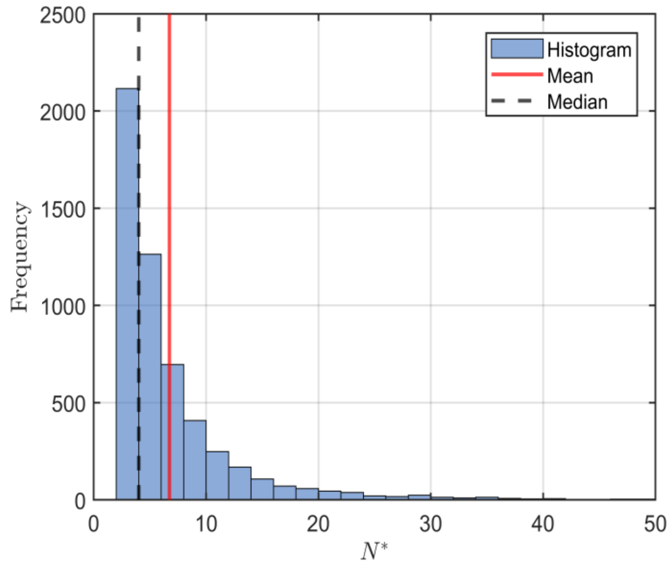

Fig. 8. Distribution of the minimum discretization level $\mathbf{N}^*$ for the three-vehicle platoon.

Table 1. Statistical distribution of the minimum discretization level N^* required for finite verification of the stability conditions.

Statistic	Leader–Follower	Three-Vehicle Platoon
Stable points analyzed	5819	5384
Minimum ($\boldsymbol{N}^*$)	1	2
Maximum ($\boldsymbol{N}^*$)	199	412
Mean ($\boldsymbol{N}^*$)	5.376	6.730
Median ($\boldsymbol{N}^*$)	3	4
Standard deviation	8.213	9.990

The statistical results reported in Table 1 support this observation. Although the maximum value increases from 199 to 412, both the mean and the median remain relatively small, indicating that high discretization levels are confined to only a limited portion of the stable parameter space.

Taken together, these results show that the finite stability criterion reproduces the previously reported stability regions while extending their characterization through the computation of the minimum discretization level required to certify each point in the controller parameter space.

4.2.4 Comparative Analysis of the Finite Stability Verification Results

Figure 9 and Table 2 compare the behavior of the finite stability criterion for the leader–follower and three-vehicle platoon configurations. The objective is to assess how the finite stability verification process evolves as the system dimension increases.

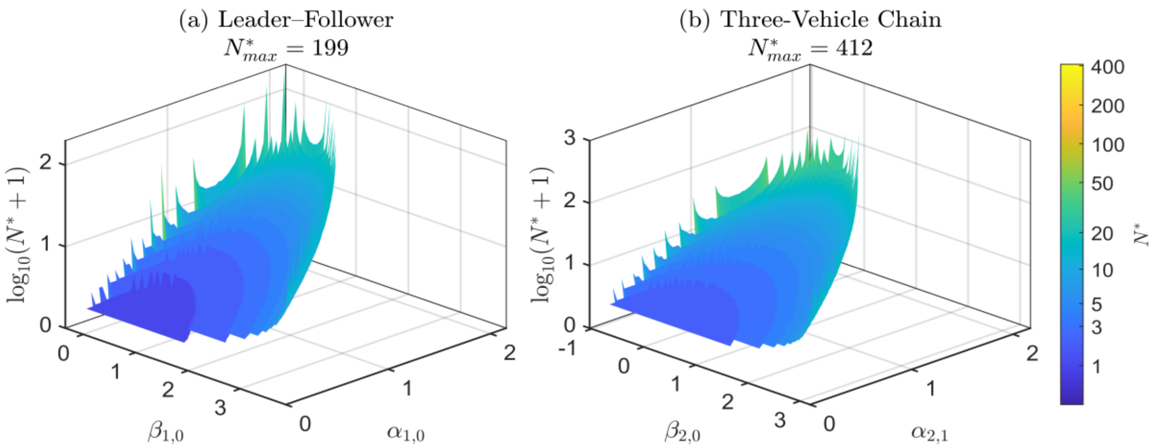

Fig. 9. Comparison of the certification index N^* for the leader–follower model and the three-vehicle platoon.

The comparison of the $N^\star$ maps shows that both configurations exhibit a similar distribution over the controller parameter space. In both cases, large values of $N^\star$ remain confined to specific regions, although the three-vehicle platoon reaches higher maximum values. This result indicates that increasing the system dimension raises the computational effort required for stability certification only for particular controller configurations.

The results reported in Table 2 support this observation. Although the system order increases from two to four states and the maximum value of $N^\star$ rises from 199 to 412, the increase in the average value remains moderate, while the number of stable operating points remains of the same order of magnitude. Taken together, these results demonstrate that the finite stability criterion remains applicable to the three-vehicle platoon and provide the basis for the experimental evaluation of the controller implemented on the connected vehicle platform.

Table 2. Finite verification results for the connected cruise control configurations considered in this work.

Metric	Leader–Follower	Three-Vehicle Platoon
System order	2	4
Stable points analyzed	5819	5384
Maximum (N^*)	199	412
Mean (N^*)	5.376	6.730
Computation time (min)	28.5	57.8
Finite verification status	Successful	Successful
Validation of previously reported stability regions	N/A	Complete agreement

Beyond reconstructing the stability regions, the proposed methodology also characterizes the numerical verification procedure through the minimum discretization level $N^\star$. Although the stability regions can be reconstructed without explicitly reporting this quantity, doing so would conceal an intrinsic property of the finite stability criterion that cannot be inferred from the stability maps alone. Consequently, the analysis of $N^\star$ provides complementary information regarding the numerical verification of the stability conditions rather than the dynamic performance of the controller (Gomez et al., 2019; Alexandrova and Belov, 2025).

For each stable operating point, $N^\star$ determines the minimum dimension of the associated finite-dimensional positivity matrix, $(n \cdot N^\star) \times (n \cdot N^\star)$, whose positive definiteness must be verified to certify the necessary and sufficient stability conditions. Therefore, $N^\star$ should not be interpreted as a controller performance index but rather as a descriptor of the finite verification procedure associated with the stability criterion.

For the connected cruise control configurations considered in this work, the relatively small values of $N^\star$, observed over most of the stable region, indicate that the stability conditions can be verified through a finite number of mathematical operations, which is consistent with the computation times reported in Table 2. Although this information is not required to identify the stability regions themselves, it provides additional insight into the numerical verification procedure associated with the finite stability criterion, thereby complementing the stability maps with information that cannot be inferred from the stability regions alone.

The comparison further shows that increasing the system order primarily affects the stability certification process rather than the overall structure of the stability regions. Although the maximum value of $N^{\star}$ increases for the three-vehicle platoon, most stable controller configurations can still be certified using relatively small discretization levels. These observations show that the computational effort required for finite stability certification is not uniformly distributed over the controller parameter space, while the overall structure of the stability regions remains essentially unchanged.

4.3 Experimental Assessment of the Controller Implementation

To assess the experimental implementation of the Connected Cruise Control (CCC) strategy, a connected vehicle platform consisting of three small-scale ground vehicles communicating through vehicle-to-vehicle (V2V) wireless links was developed. The implemented controller gains were selected from the stable regions identified by the finite stability criterion, using $(\alpha_{1,0}, \beta_{1,0}) = (0.6, 0.7)$ for the leader–follower configuration and $(\alpha_{2,1}, \beta_{2,0}, \beta_{2,1}) = (0.6, 0.7, 0.7)$ for the three-vehicle platoon.

The experiments are intended to evaluate the performance of the implemented controller on a physical connected vehicle platform operating around the equilibrium conditions considered in the mathematical model. In contrast, the validation of the finite stability criterion is provided by the theoretical analysis presented in the previous sections.

4.3.1 Experimental Platform

The experimental platform employed in this work is shown in Fig. 10. It consists of three small-scale ground vehicles designed to implement the Connected Cruise Control strategy in a distributed manner. Each vehicle integrates the hardware required to execute the control law locally, measure the inter-vehicle spacing, estimate the longitudinal velocity, and exchange information with preceding vehicles through V2V wireless communication. The platform is based on Arduino Uno microcontrollers, NRF24L01 wireless communication modules, HC-SR04 ultrasonic sensors for inter-vehicle spacing measurements, optical encoders for longitudinal velocity estimation, and RoboClaw 2×30A motor controllers for vehicle actuation.

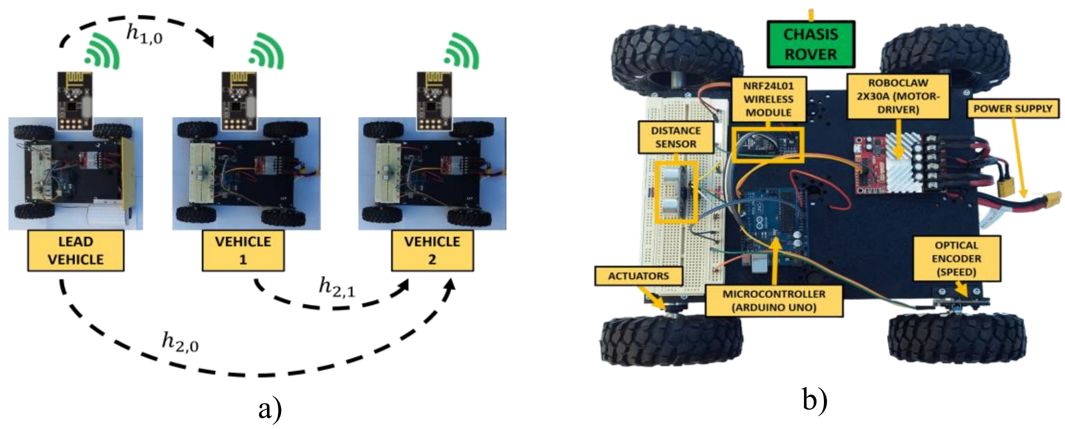

Fig. 10. (a) Experimental three-vehicle connected platoon used for validation of the finite verification framework. Communication delays are denoted by $\mathbf{h_{1,0}}$, $\mathbf{h_{2,0}}$ and $\mathbf{h_{2,1}}$. (b) Experimental vehicle platform including the microcontroller, wireless communication module, distance sensor, optical encoder, motor driver, and power supply.

The V2V communication architecture provides each vehicle with the predecessor velocity information required by the control law, following the communication topology shown in Fig. 11. Throughout the experiments, a sampling period of 250 ms was employed, with approximately uniform communication delays of $h_{1,0} = h_{2,0} = h_{2,1} = 0.30\ s$. The reference inter-vehicle spacing was set to $d^{\star} = 0.75\ m$, while the equilibrium speed was fixed at $v^{\star} = 0.654\ m/s$. Under these operating conditions, the experimental results presented in the following subsection were obtained.

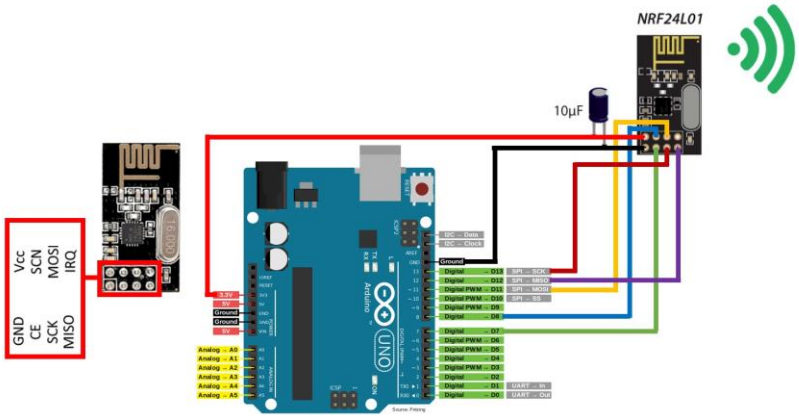

Fig. 11. Wireless communication interface based on the NRF24L01 transceiver module used for vehicle-to-vehicle information exchange.

4.3.2 Experimental Evaluation of the Controller

This experimental evaluation assesses the performance of the Connected Cruise Control strategy using the controller gains selected from the stability regions identified in Sections 4.1 and 4.2. The experiments were conducted by imposing speed variations on the leader vehicle, whose reference speed $v^{\star}$ was tracked using a PID controller. The follower vehicles implemented the Connected Cruise Control strategy using the controller gains selected in Sections 4.1 and 4.2. Figures 12–14 present, respectively, the longitudinal velocity responses, the inter-vehicle spacings, and the implementation variables (tracking errors and control signals) recorded during the experiments.

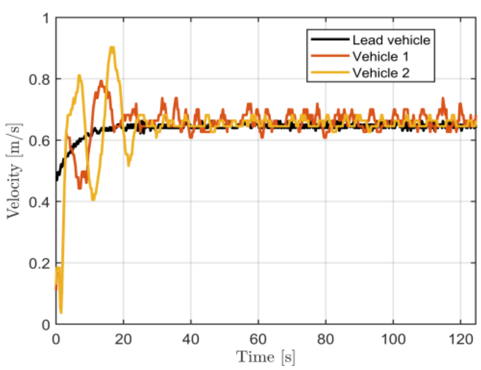

Fig. 12. Experimental velocity tracking performance of the connected vehicle platoon.

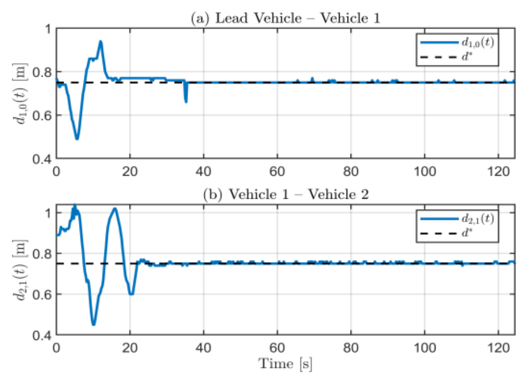

Fig. 13. Experimental inter-vehicle distances. (a) Distance between the lead vehicle and Vehicle 1. (b) Distance between Vehicle 1 and Vehicle 2.

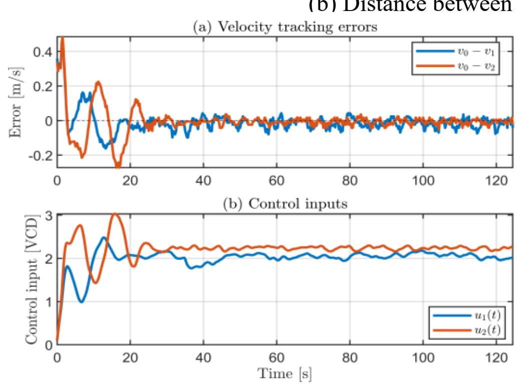

Fig. 12. Experimental tracking errors and control inputs. (a) Velocity tracking errors. (b) Control actions applied to Vehicle 1 and Vehicle 2.

The experimental responses show that the follower vehicles successfully reproduce the velocity variations imposed by the leader while maintaining the inter-vehicle spacings around their reference values throughout the experiments. Moreover, the tracking errors remain bounded, and the control signals evolve smoothly without evidence of actuator saturation or abrupt control actions.

Taken together, these results demonstrate that the controller gains selected from the stability regions identified by the finite stability criterion can be successfully implemented on a connected vehicle platform operating around the equilibrium conditions considered in the mathematical model. In this sense, the stability regions provide a systematic basis for controller gain selection, whereas the minimum discretization level $N^{\star}$ complements this process by quantifying the computational effort required to certify each controller configuration through necessary and sufficient stability conditions. Consequently, the proposed procedure integrates finite stability certification, controller gain selection, and experimental implementation into a unified framework for the design of Connected Cruise Control systems.

5 Conclusions

This work demonstrates that recent advances in finite stability criteria based on the Delay Lyapunov Matrix can be effectively incorporated into the stability analysis of linear models of Connected Cruise Control systems, enabling their stability to be analyzed through finite necessary and sufficient stability conditions. Beyond reproducing previously reported stability regions, the proposed analysis provides an additional characterization of the controller parameter space through the minimum discretization level required for finite stability verification, complementing the classical stability maps with information on the verification requirements associated with each stable operating point.

The experimental implementation complements the numerical analysis by demonstrating the feasibility of deploying controller gains obtained from the finite stability analysis on a connected vehicle platform under operating conditions consistent with the theoretical model.

The integration of finite delay Lyapunov matrix-based stability criteria into the analysis of Connected Cruise Control systems opens new opportunities for extending these methods to a broader class of time-delay systems, alternative control architectures, and the development of computational tools that facilitate their practical application.

References

Alexandrova, I. V., & Belov, A. I. (2025). Synthesis of discretized Lyapunov functional method and the Lyapunov matrix approach for linear time delay systems. *Automatica, 171*, 111793. https://doi.org/10.1016/j.automatica.2024.111793

Bellman, R., & Cooke, K. L. (1963). *Differential-difference equations*. Academic Press.

Cuvas-Castillo, C., Castaño-Hernández, A., & Ordaz-Oliver, J. P. (2019). An efficient algorithm for the construction of a block matrix depending on the delay Lyapunov matrix for testing stability of time-delay systems. In *2019 16th International Conference on Electrical Engineering, Computing Science and Automatic Control (CCE)* (pp. 1–5). IEEE. https://doi.org/10.1109/ICEEE.2019.8884539

Gomez, M. A., Egorov, A. V., & Mondié, S. (2019). Lyapunov matrix based necessary and sufficient stability condition by finite number of mathematical operations for retarded type systems. *Automatica, 108*, 108475. https://doi.org/10.1016/j.automatica.2019.06.027

Juárez, L., Mondié, S., & Cuvas, C. (2018). Connected cruise control of a car platoon: A time-domain stability analysis. *Proceedings of the Institution of Mechanical Engineers, Part I: Journal of Systems and Control Engineering, 232*(6), 672–682. https://doi.org/10.1177/0959651818766224

Kharitonov, V. L. (2013). *Time-delay systems: Lyapunov functionals and matrices*. Birkhäuser. https://doi.org/10.1007/978-0-8176-8367-2

Mondié, S., Egorov, A. V., & Gomez, M. A. (2022). Lyapunov stability tests for linear time-delay systems. *Annual Reviews in Control, 54*, 68–80. https://doi.org/10.1016/j.arcontrol.2022.09.001

Orosz, G. (2016). Connected cruise control: Modelling, delay effects, and nonlinear behaviour. *Vehicle System Dynamics, 54*(8), 1147–1176. https://doi.org/10.1080/00423114.2016.1193209

Rajamani, R. (2012). *Vehicle dynamics and control* (2nd ed.). Springer. https://doi.org/10.1007/978-1-4614-1433-9

Treiber, M., & Kesting, A. (2013). *Traffic flow dynamics: Data, models and simulation*. Springer. https://doi.org/10.1007/978-3-642-32460-4

Acknowledgments: The authors would like to thank the anonymous reviewers for their valuable comments and suggestions, which helped improve the quality of this manuscript.

Data Availability Statement: The data supporting the findings of this study are available from the corresponding author upon reasonable request.

Conflicts of Interest: The authors declare no conflicts of interest.